MHD Stability Analysis and Global Mode Identification Preparing for High Beta Operation in KSTAR*

Y.S. Park[1], S.A. Sabbagh[1], J.W. Berkery[1], Y. Jiang[1], J.H. Ahn[1], J.G. Bak[2], J.M. Bialek[1], H.S. Han[2], B.H. Park[2], Y.M. Jeon[2], J. Kim[2], S.H. Hahn[2], J.H. Lee[2], W.H. Ko[2], J.S. Ko[2], Y.K. In[2], S.W. Yoon[2], J.G. Kwak[2], Y.K. Oh[2], Z. Wang[3], N.M. Ferraro[3], C.E. Myers[3], S.C. Jardin[3], A.H. Glasser[4], G.S. Yun[5]

[1]Department of Applied Physics, Columbia University, New York, NY, USA
[2]National Fusion Research Institute, Daejeon, Korea
[3]Princeton Plasma Physics Laboratory, Princeton, NJ, USA
[4]U. Washington, Seattle, WA, USA
[5]POSTECH, Pohang, Korea

NSTX-U Physics Meeting
November 30, 2017
PPPL, Princeton, NJ

In collaboration with

NFRI National Fusion Research Institute
PPPL UNIST
POSTECH

KSTAR

*Work supported by the U.S. Department of Energy under contract DE-FG02-99ER54524 and DE-SC0016614

KSTAR H-mode equilibria have reached and exceeded the computed n = 1 ideal no-wall stability limit

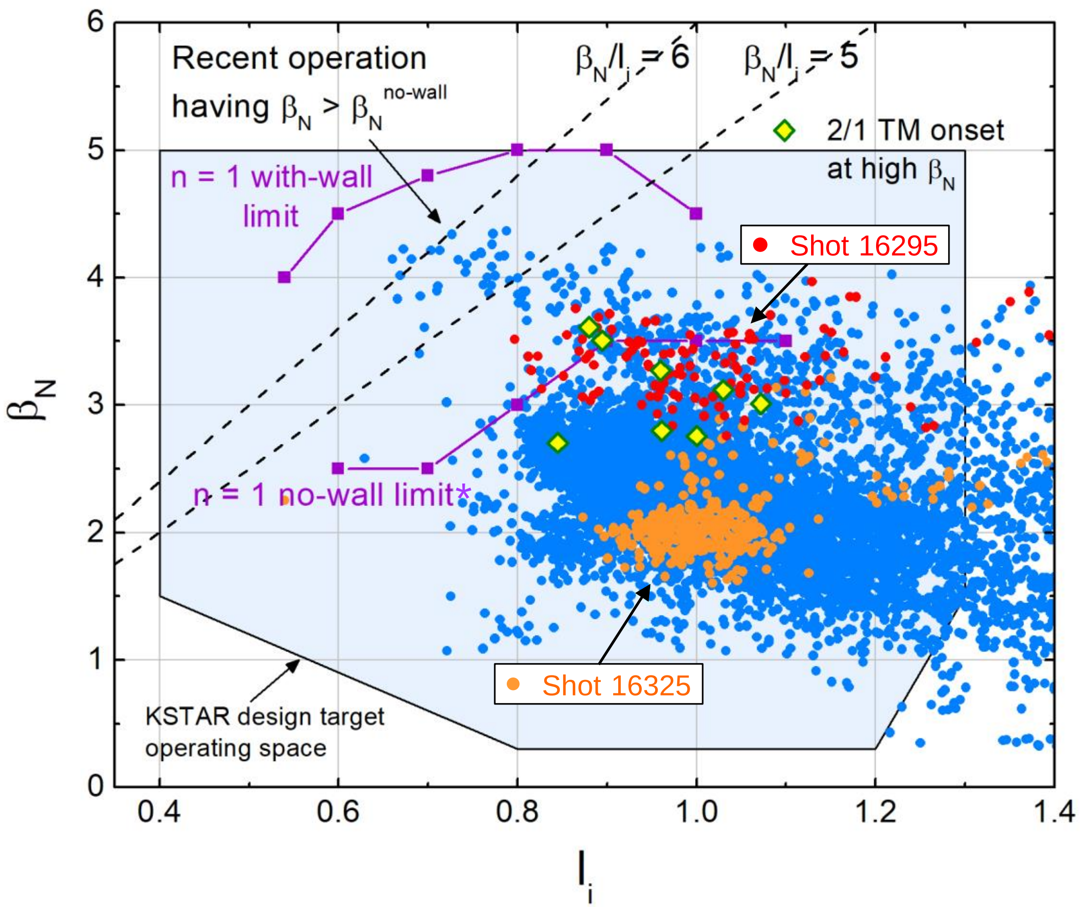

Normalized beta vs. internal inductance from EFIT reconstruction** containing ~9,000 equilibria produced in the 2016 device campaign

*O. Katsuro-Hopkins, *et al*., Nucl. Fusion **50** (2010) 025019

** Y.S. Park, *et al*., Nucl. Fusion **53** (2013) 083029

- Parameters for high β_N
  - B_T in range 0.9-1.3 T
  - P_{NBI} = 4.5-5.5 MW
- Highest $\beta_N = 4.3$, $\beta_N/l_i > 6$
- MHD stability at high β_N
  - Many equilibria operate above the published ideal n = 1 no-wall stability limit (DCON)
  - Plasma is subject to RWM instability, depending on plasma rotation profile
  - High $\beta_N > \beta_N^{no\text{-}wall}$ operation mostly limited by 2/1 mode

High β_N > 3 equilibria limited by MHD - shot 16295

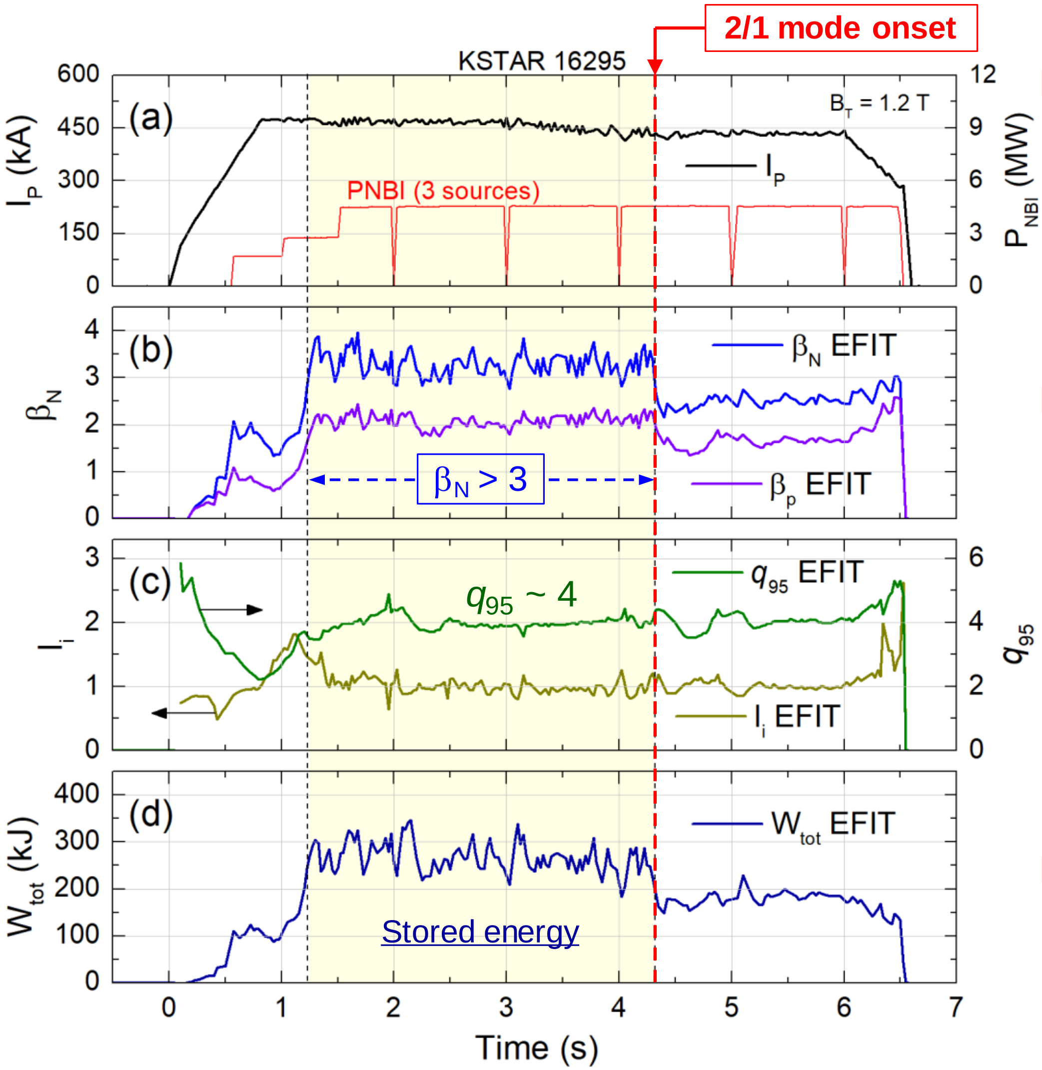

KSTAR high β_N discharge evolution showing parameters from fully converged EFIT reconstructions

- High β_N plasmas were significantly extended to longer pulse by utilizing improved plasma control
- Sustained high β_N^{avg} = 3.3 achieved for 3 s
  - Used max. available P_{NBI} = 4.5 MW
  - I_p = 430-470 kA, B_T = 1.2 T, q_{95} = 4.0-4.5, W_{tot} = 270 kJ
- 2/1 tearing mode onset at high β_N phase
  - Consequently reduces β_N and W_{tot} by ~35%

Onset of strong 2/1 tearing mode terminated high β_N

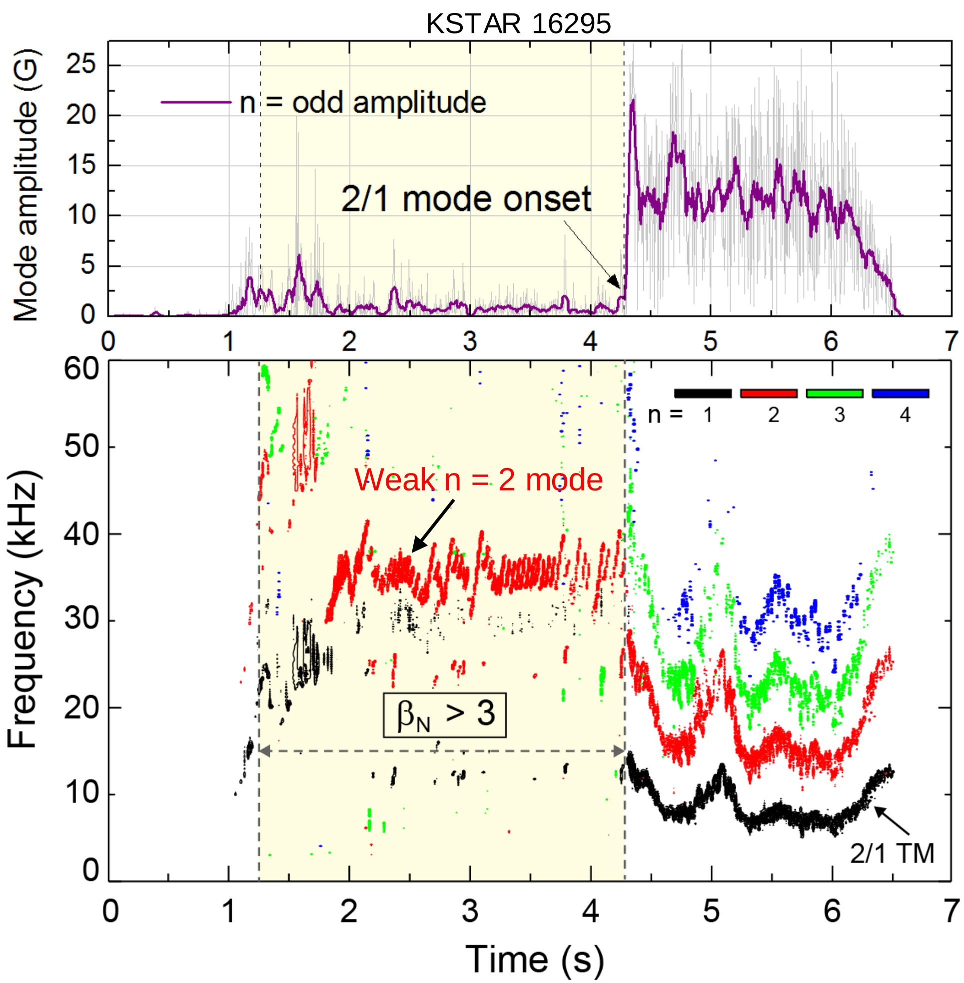

Toroidal magnetic probe spectrum and mode amplitude in high β_N discharge

- At high β_N phase, a benign n = 2 mode (presumably 3/2 mode) exists with strong sawteeth
  - No indication of W_{tot} reduction due to the n = 2 mode having $|\tilde{B}_p|$ ~ 2 G
- High β_N operation was limited by strong 2/1 tearing mode onset
  - Measured mode amplitude > 20 G
  - Both W_{tot} and β_N were reduced by ~35% but maintained H-mode
  - Similar discharges exhibited different 2/1 tearing mode onset time (expected to be triggered by sawteeth)
- Plasma rotation profile significantly reduced by > 20% due to the 2/1 mode onset

Comparative equilibria having higher q_{95} and β_p shows very different MHD stability - shot 16325

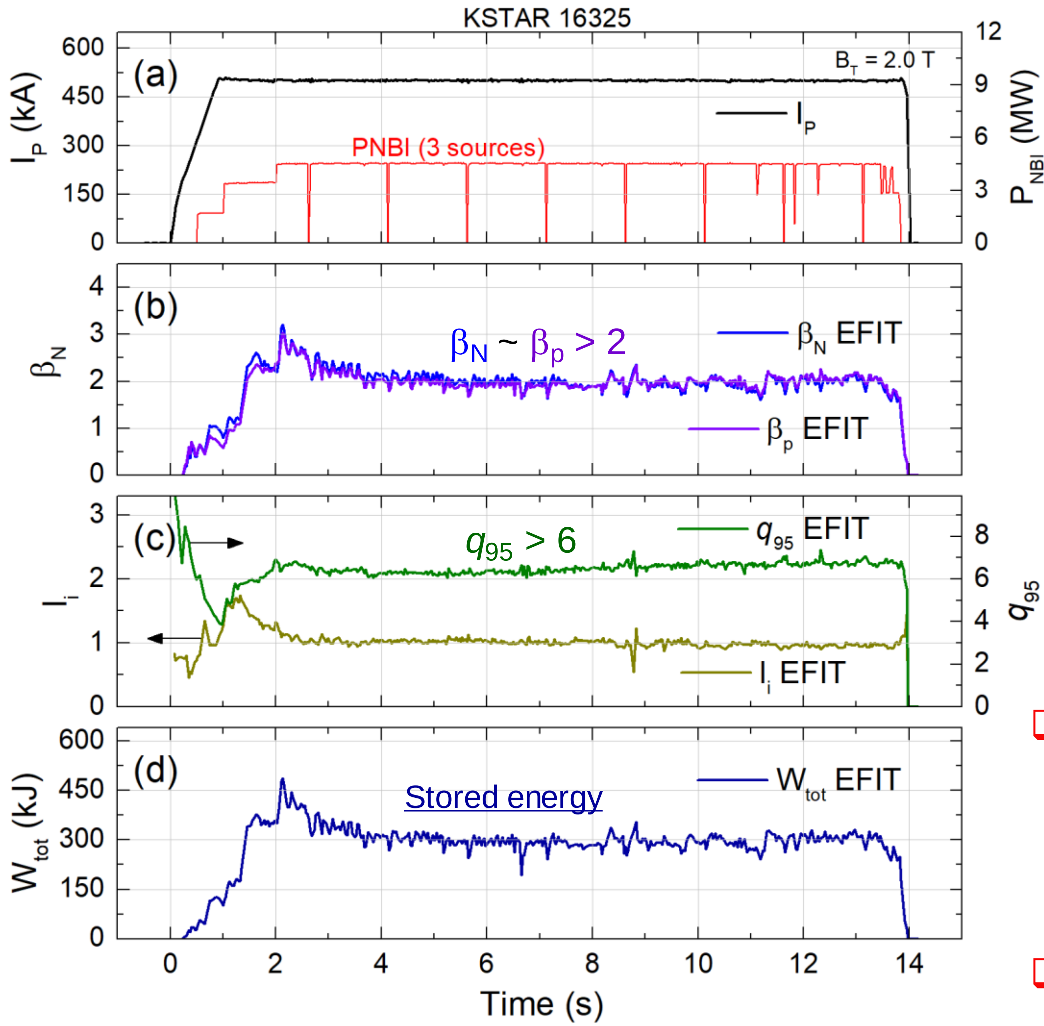

KSTAR 16325 discharge evolution showing parameters from fully converged EFIT reconstructions

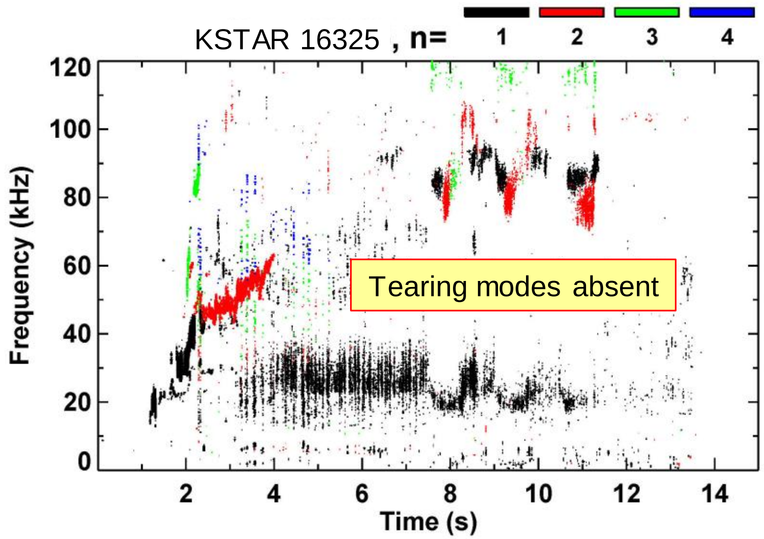

Toroidal magnetic probe spectrum

- Plasma operation at elevated B_T produced equilibria having higher q_{95} and β_p
- Unlike shot 16295, discharge doesn't experience any major beta-limiting MHD activities

Kinetic EFIT with MSE constraints used for accurate stability analysis for the first time on KSTAR

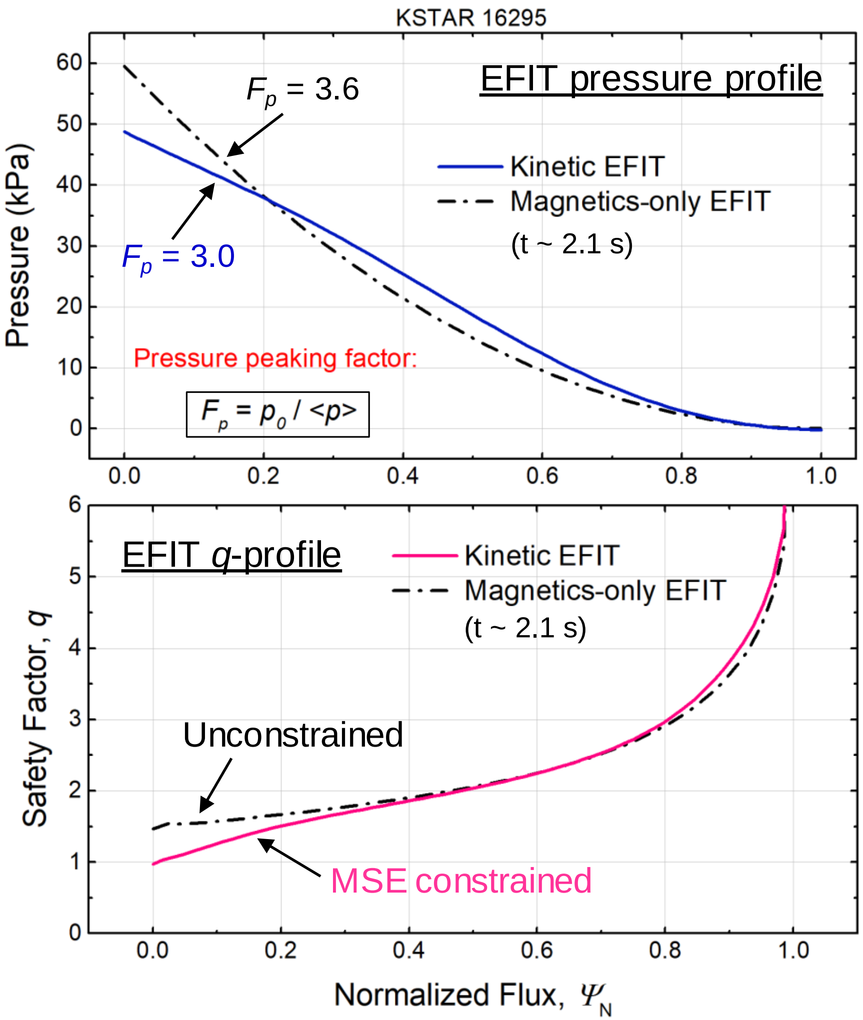

Reconstructed pressure and safety factor profile from kinetic EFIT using internal profile constraints

- Equilibrium reconstruction now uses measured internal profile constraints
  - Provides reliable pressure profile and internal magnetic geometry necessary for stability and transport studies

    S.A. Sabbagh, Nucl. Fusion **41** (2001) 1601
- KSTAR is equipped with key internal profile diagnostics
  - Charge exchange (T_i, V_ϕ) : 32 CHs
  - Thomson scattering (T_e, n_e) : 27 CHs
  - ECE radiometer (T_e) : 76 CHs
  - Motional Stark Effect : 25 CHs
  - Total number of available constraints for fit : 161 magnetics + 160 kinetics & MSE

SEE Y. Jiang's talk on 11/29/17

DCON stability calculation shows high β_N equilibria are subject to n = 1 ideal instability

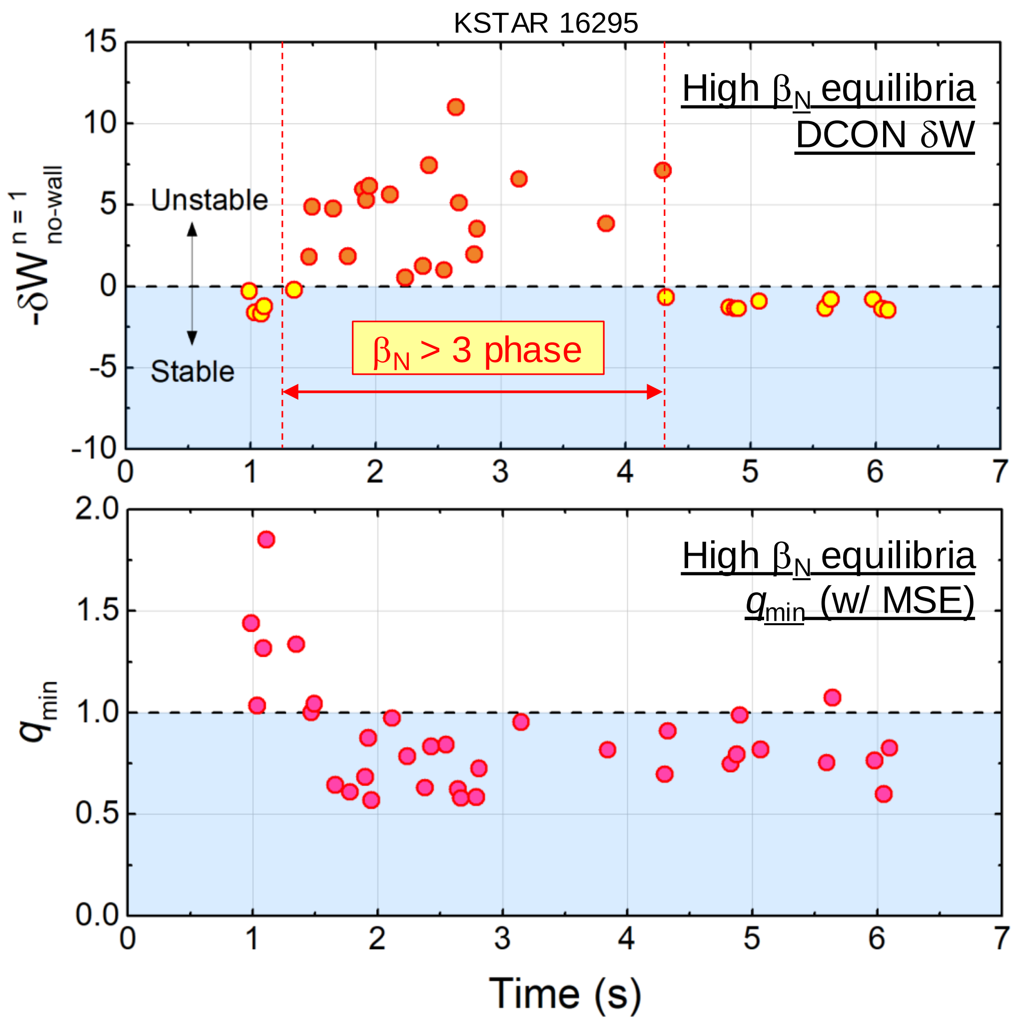

DCON computed no-wall δW and EFIT q_{min} in high β_N equilibria of shot 16295

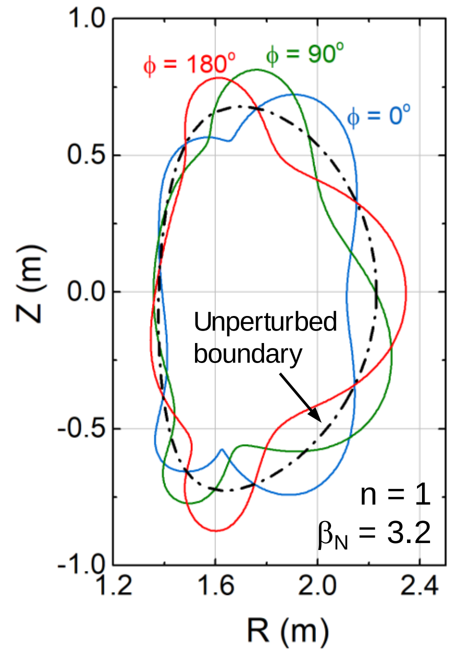

DCON computed δB_n of unstable n = 1 mode at t = 2.356 s

- At observed high β_N phase, DCON calculates unstable n = 1 mode with no-wall ($\beta_N > \beta_N^{\text{no-wall}}$)
- q_{min} mostly stays below 1 which supports a potential 2/1 mode triggering by sawteeth

A.H. Glasser, Phys. Plasmas **23** (2016) 072505

Ideal mode stability computed by M3D-C¹ code shows consistent result with DCON

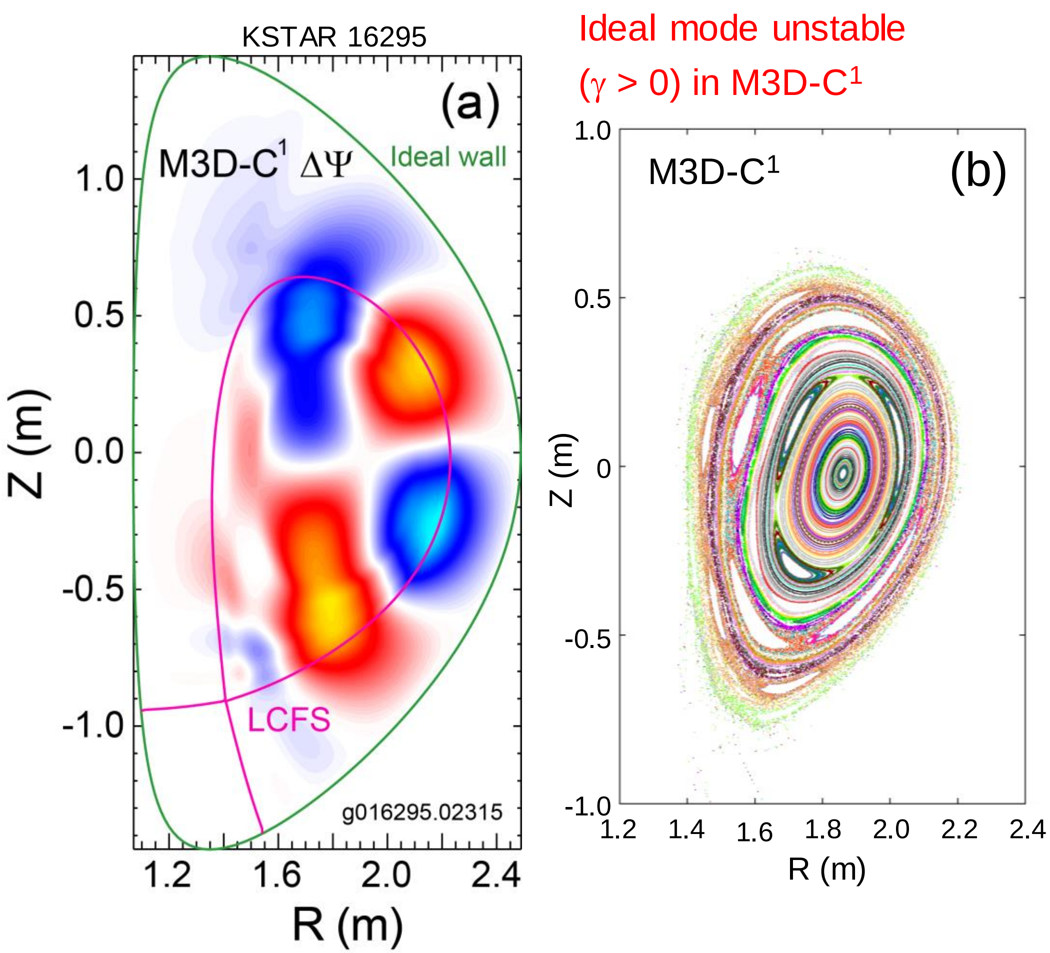

(a) The perturbed poloidal flux of unstable ideal mode from M3D-C¹ and (b) corresponding Poincaré plot with exaggerated displacement

- Linear stability of ideal mode computed by using resistive MHD code M3D-C¹
  - Extended MHD code solving two-fluid resistive MHD equations
- The high β_N equilibrium is computed to be unstable by M3D-C¹ consistent with DCON
- Kinetic RWM stability can explain the observed RWM stable operation at $\beta_N > \beta_N^{no\text{-}wall}$

Comparative equilibria with high q_{95} are stable to n = 1 in DCON

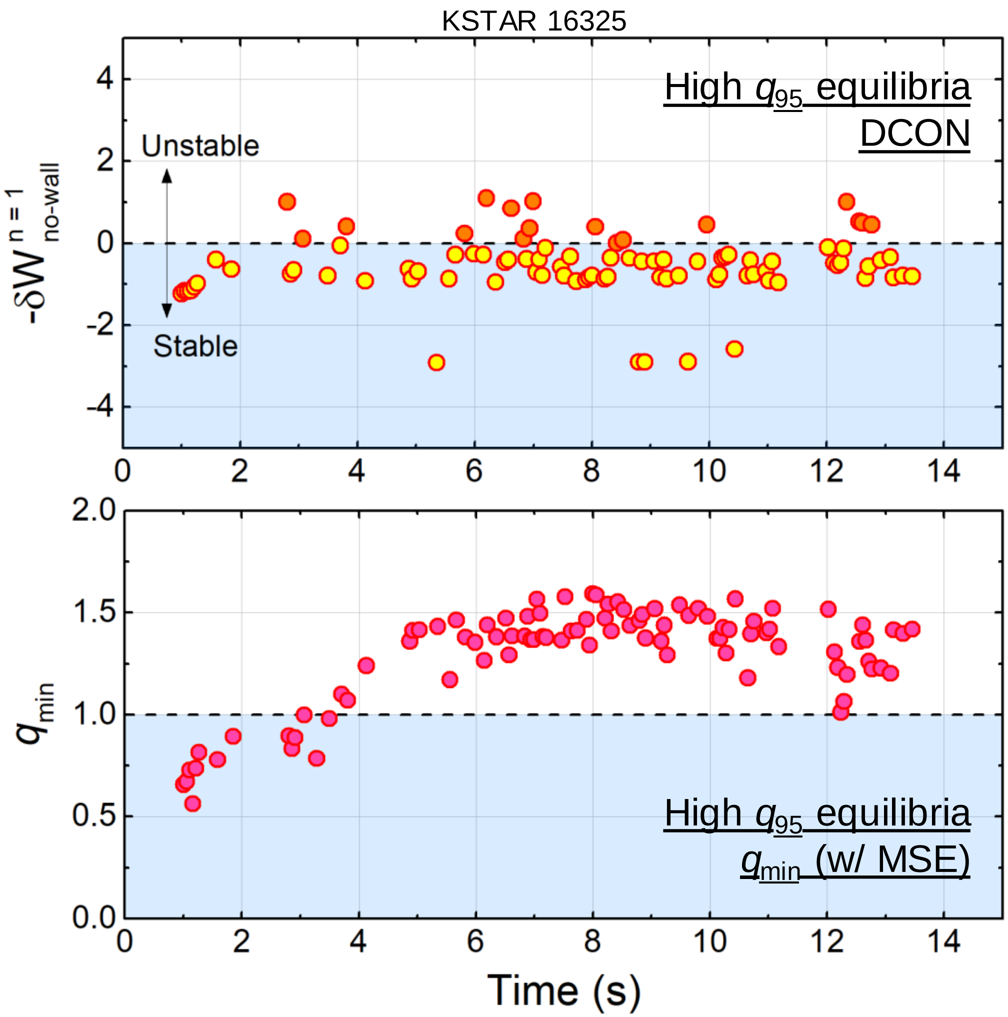

DCON computed no-wall δW and EFIT q_{min} in high q_{95} equilibria of shot 16325

- Unlike the high β_N case, equilibria at lower β_N is mostly stable to n = 1 ideal modes in DCON
- The elevated q-profile at higher B_T leads to higher q_{min} above 1
  - No indication of sawteeth found in the MHD spectrogram
  - Possible lack of non-linear seeding from sawteeth could improve the neoclassical tearing mode stability

Tearing stability is examined by the resistive DCON code

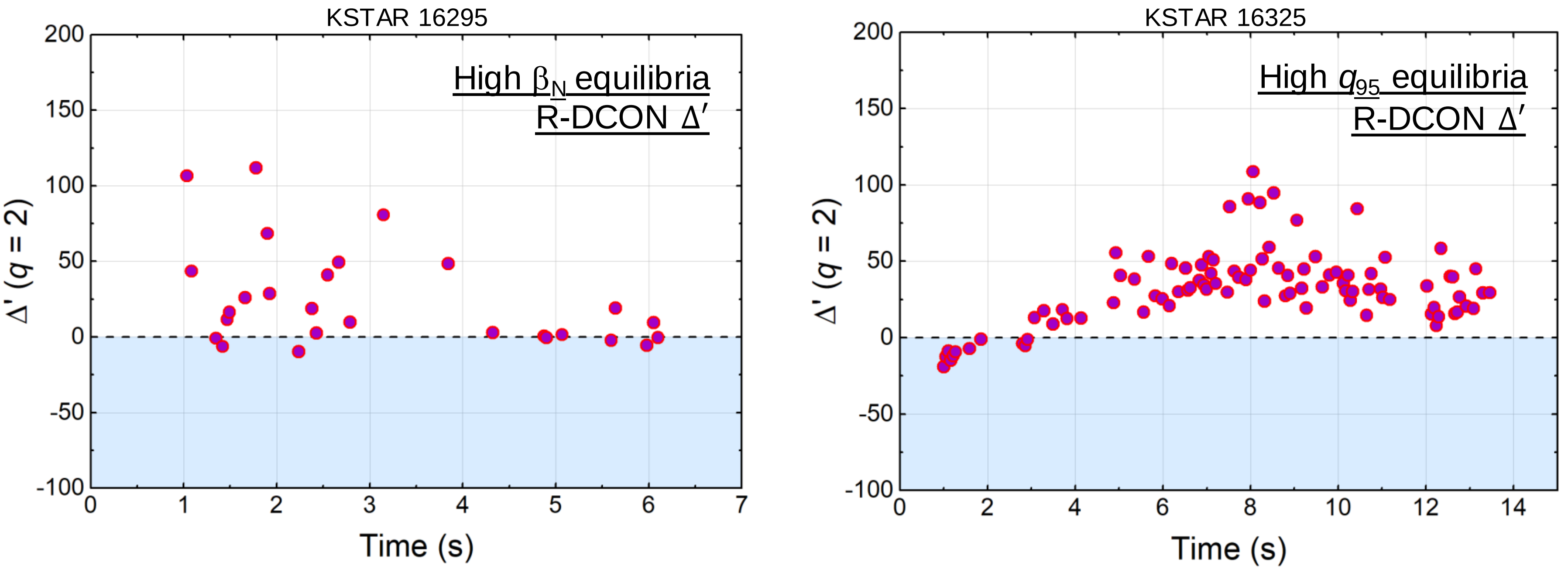

- Resistive DCON is used to compute the tearing stability index, Δ', at q = 2 surface by using the outer layer solutions
- Δ' which is mostly positive in the target equilibria predicts unstable tearing mode, and explains the importance of the neoclassical effects in the observed stability

A.H. Glasser, *et al.*, Phys. Plasmas **23** (2016) 112506

Resistive 2/1 tearing mode stability of high β_N equilibria examined by using M3D-C1

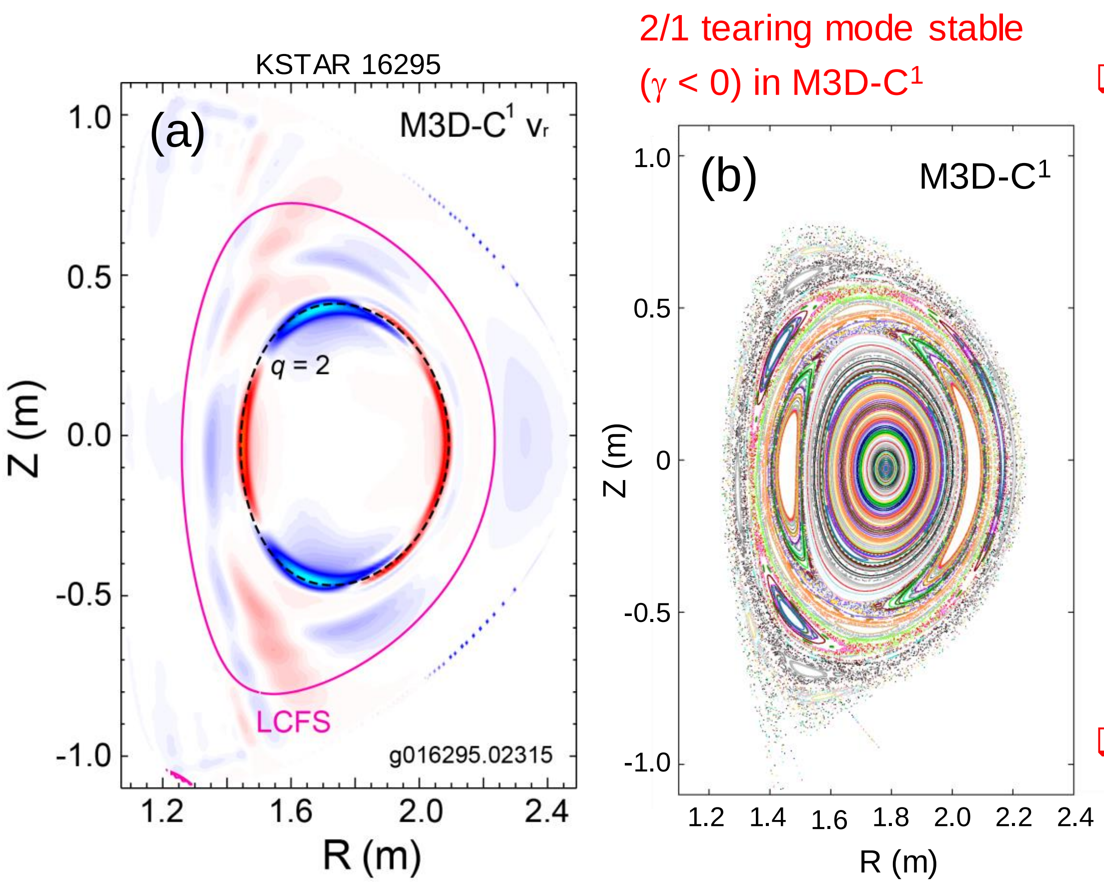

(a) The radial velocity eigenfunction of a 2/1 tearing mode from M3D-C1 and (b) corresponding Poincaré plot with exaggerated displacement

S.C. Jardin, *et al*., J. Comput. Phys. **226** (2007) 2146

- Linear stability of the observed 2/1 tearing mode computed by M3D-C1
  - Used experimental equilibrium and measured T_e profile from TS diagnostic for the input resistivity
  - Increased resolution around the mode rational surface using the adaptive meshing
- The 2/1 tearing mode is marginally stable in M3D-C1
  - Unstable experimentally
  - Computed negative mode growth rate

TRANSP analysis examines j_{BS}-profile alignment with tearing rational surface

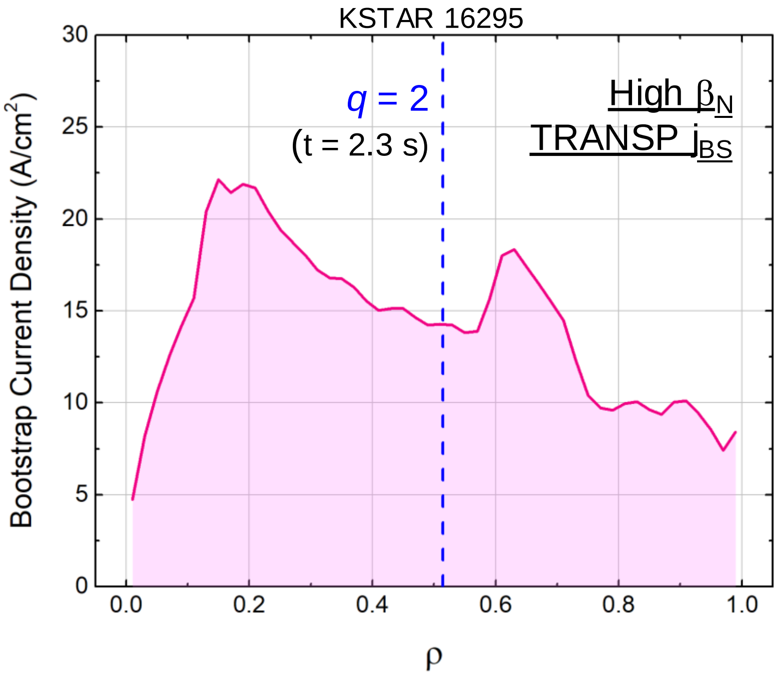

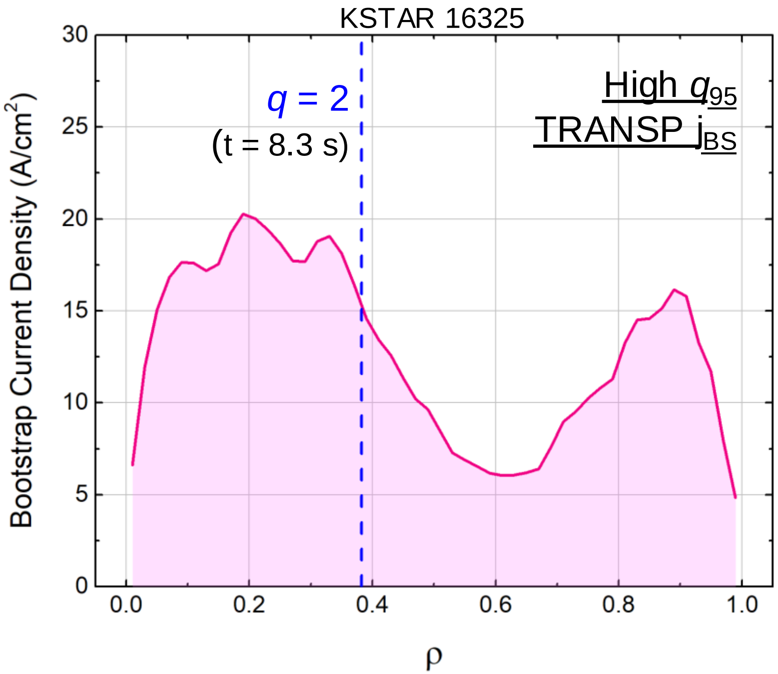

- Interpretive TRANSP analysis using KSTAR experimental equilibria and measured internal profiles to calculate plasma evolutions especially for the non-inductive plasma current
- Bootstrap current profile from TRANSP and *q*-profile from MSE-constrained EFIT will be used for improved tearing stability analysis including the pressure-driven terms

SEE J.H. Ahn's talk on 11/29/17

RWM stability evaluated with ideal and kinetic components allows for passive stabilization of the RWM

- Kinetic effects modify ideal MHD n = 1 stability (MISK code)
  - Collisional dissipation
  - Rotational stabilization

kinetic modification

$$(\gamma - i\omega_r)\tau_w = -\frac{\delta W_\infty + \boxed{\delta W_K}}{\delta W_b + \boxed{\delta W_K}}$$

B. Hu, *et al*., PRL **93** (2004) 105002
J.W. Berkery, *et al*., PRL **104** (2010) 035003
S.A. Sabbagh, *et al*., Nucl. Fusion **50** (2010) 025020

<u>Trapped ion component (typically dominates Re(δW_K))</u>

$$\delta W_K \propto \int \left[\frac{\omega_{*N} + \left(\hat{\varepsilon} - \tfrac{3}{2}\right)\omega_{*T} + \omega_E - \omega - i\gamma}{\langle \omega_D \rangle + l\omega_b - i\nu_{eff} + \omega_E - \omega - i\gamma} \right] \hat{\varepsilon}^{\frac{5}{2}} e^{-\hat{\varepsilon}} d\hat{\varepsilon}$$

precession drift | bounce | collisionality | E×B

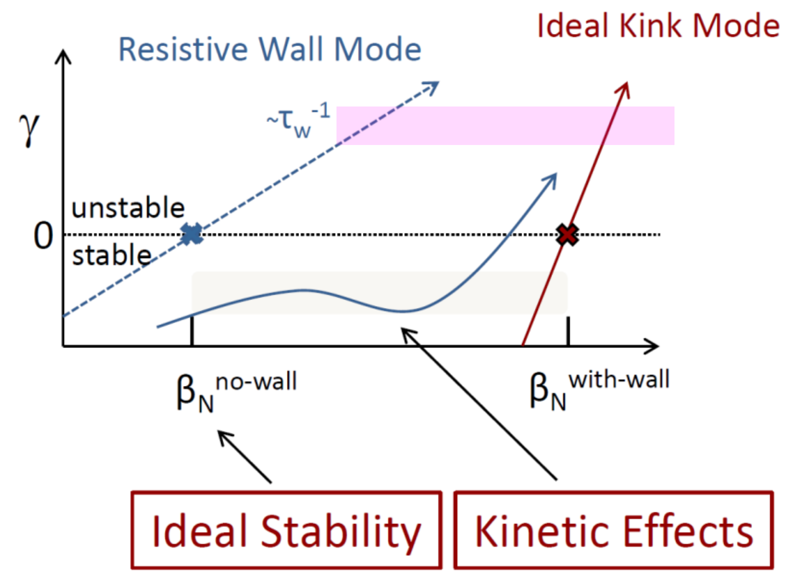

J.W. Berkery, *et al*., MHD Workshop (2015)

- Stability modification depends on
  - Integrated ω_ϕ profile: resonances in δW_K
  - Particle collisionality

- Plasma is stable when rotation is in resonance
  - l = 0 harmonic : resonance with precession drift frequency $\boxed{\omega_E + <\omega_D> = 0}$
  - l = -1 harmonic : resonance with bounce frequency $\boxed{\omega_E + <\omega_D> - \omega_b = 0}$

Kinetic modification of RWM stability is evaluated with including energetic particle effects

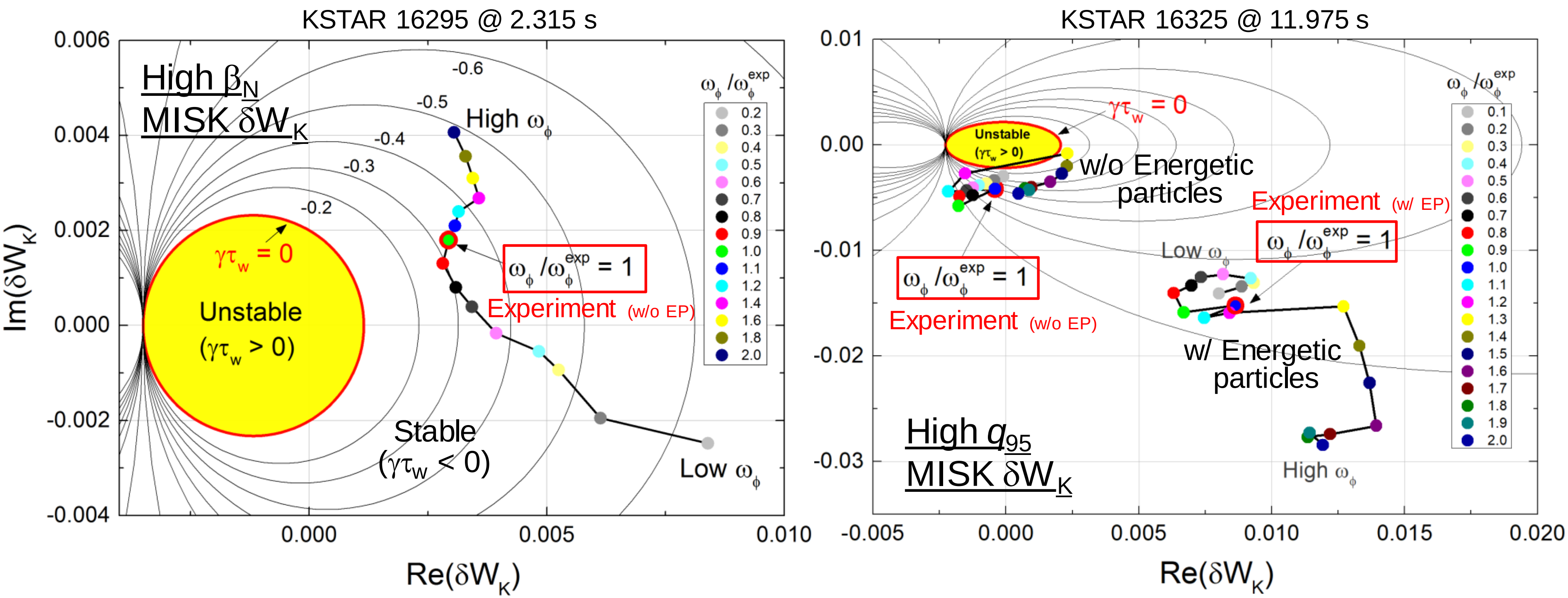

n = 1 RWM stability diagram with scaled experimental rotation profiles

- MISK calculations find the equilibrium is stable to RWM as is consistent with experiment (rotation profile is scaled from 0.1 to 2 times in the analysis)
- Energetic particles are predicted to give a strong stabilizing effect to RWMs

J.W. Berkery, *et al*., PRL **104** (2010) 035003
Y.S. Park, *et al*., Nucl. Fusion **51** (2011) 053001

RWM active control system hardware is installed in KSTAR

KSTAR RWM feedback model in VALEN-3D

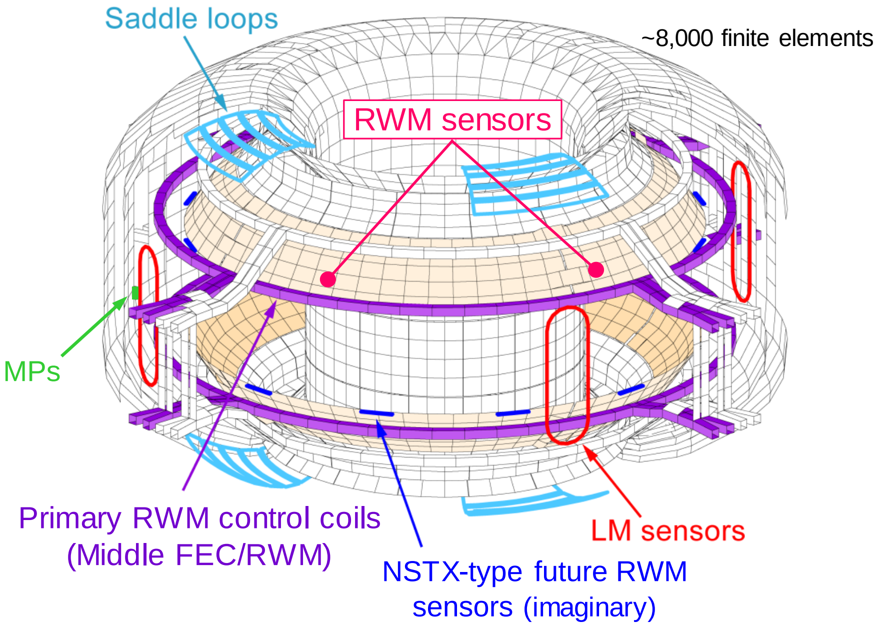

Y.S. Park, *et al*., Phys. Plasmas **21** (2014) 012513

RWM feedback sensors on passive plates

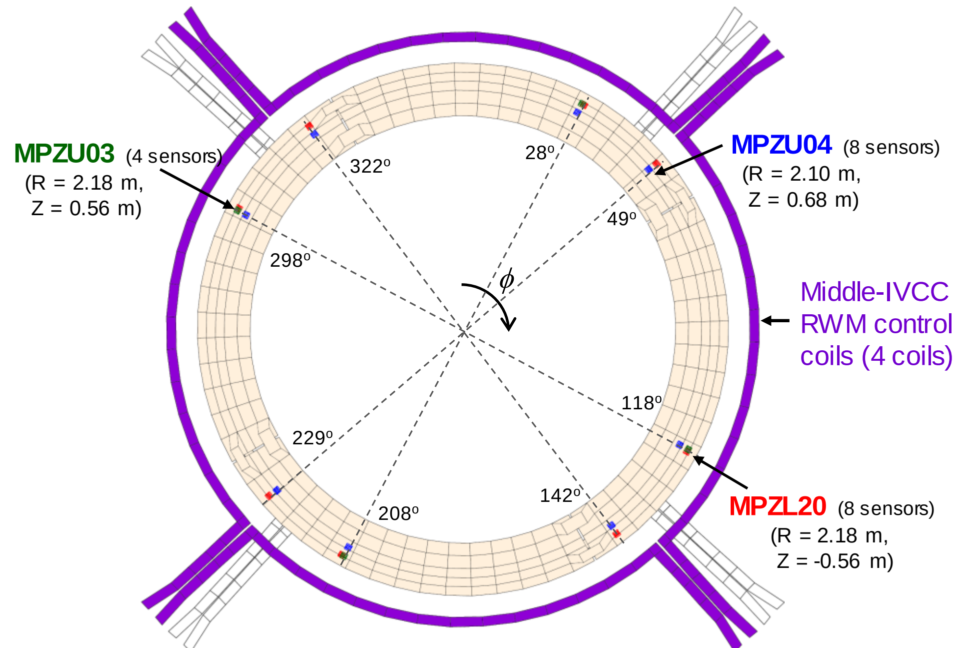

<lower passive plate - top view>

- For plasma operation at $\beta_N > \beta_N^{\text{no-wall}}$, RWM control system is prepared in KSTAR
  - The middle in-vessel control coils (IVCCs) minimizes the inductive shielding by the copper passive stabilizing plates during RWM feedback
  - Three sets of RWM B_p sensors with max. 8 toroidal locations (Upper – MPZU03 & MPZU04, and Lower – MPZL20) have been installed on the inner surface of the passive plates ⇒ total 20 independent B_p measurements for RWM identification (f_{sample} = 20 kHz)

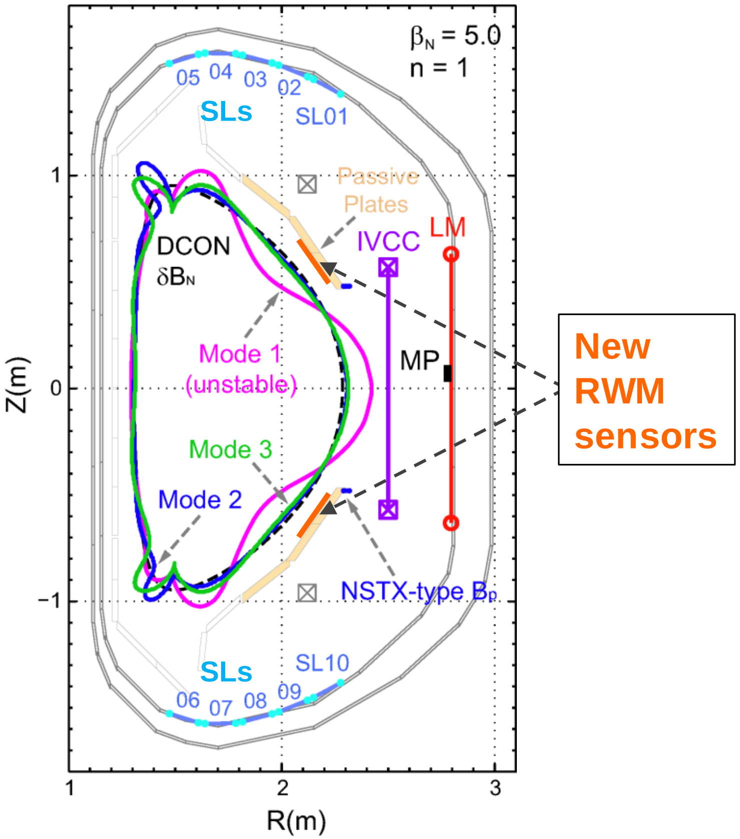

Y.S. Park, *et al*., Phys. Plasmas **21** (2014) 012513

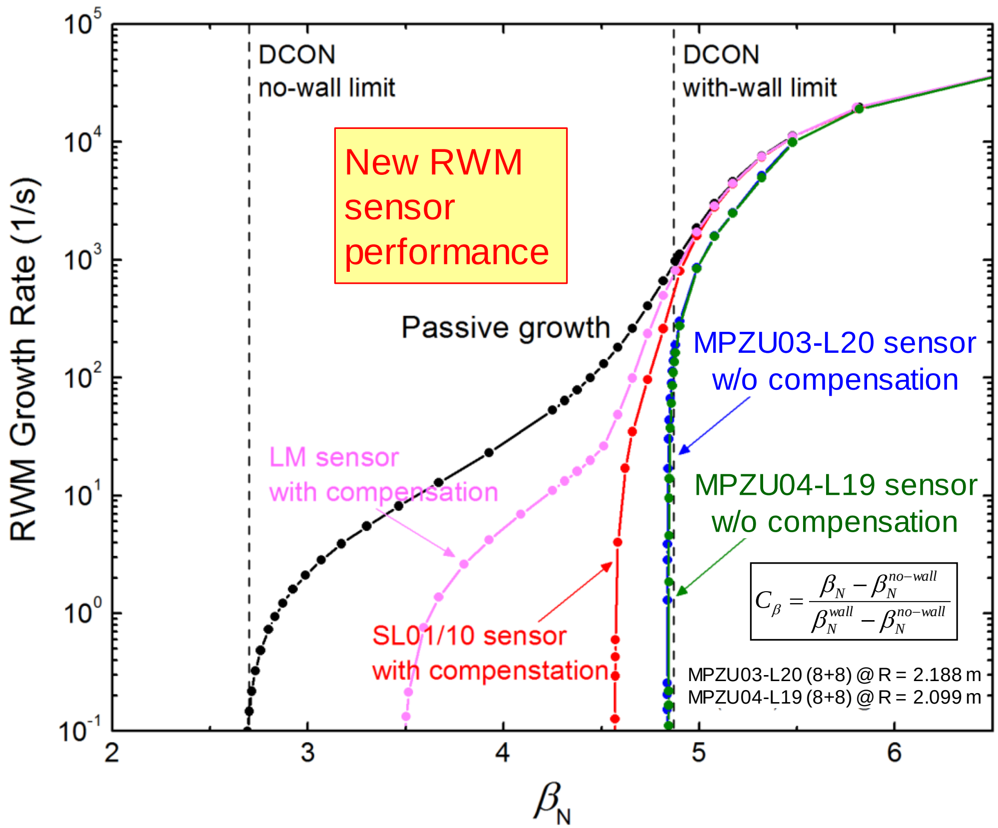

RWM control performance of the new RWM sensors

- The design advantages of the new RWM sensors result in greater mode control - almost up to the ideal with-wall limit (C_β = 98%, β_N = 4.8)

Strong coupling between RWM feedback sensors and passive plates could be detrimental to RWM feedback

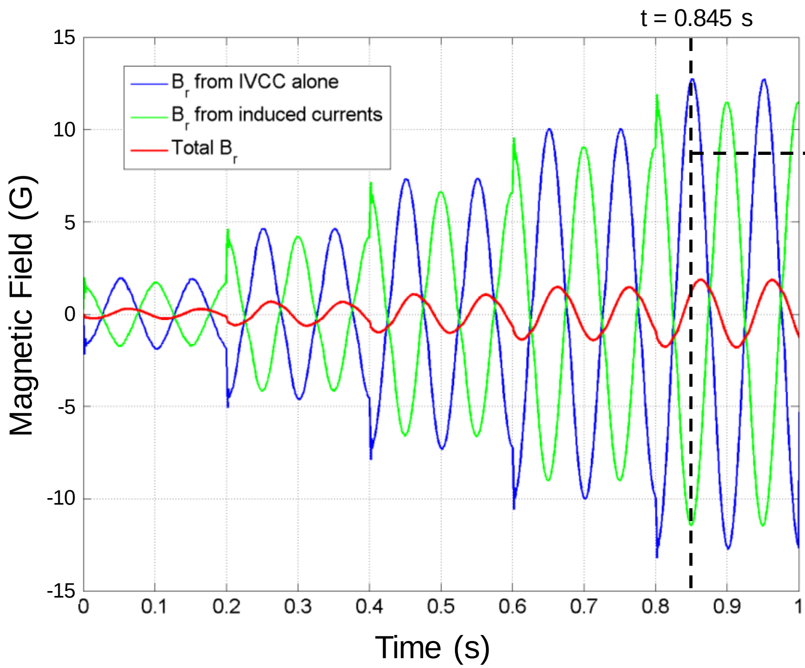

VALEN-3D computed sensor measurement

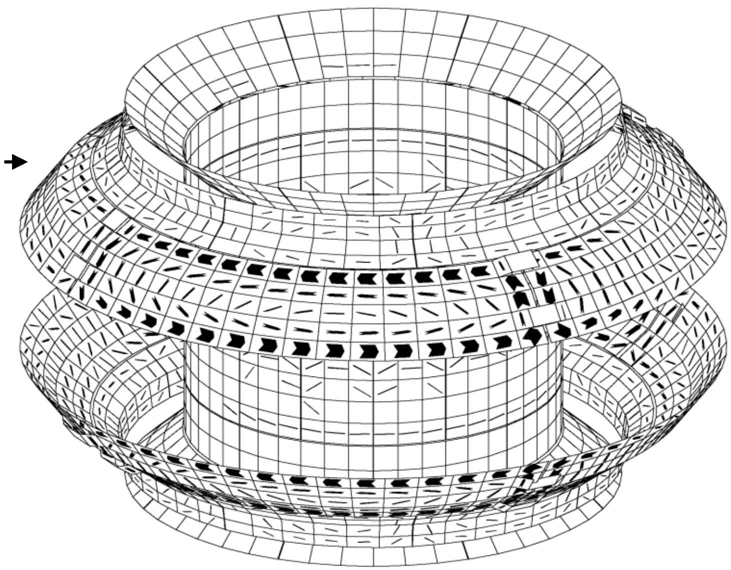

Computed induced currents on the internal passive conductors when 10 Hz n = 1 rotating field is applied from RWM control coils (m-IVCCs)

- Transient effects of the induced currents on the passive plates have been examined by VALEN-3D code
- KSTAR passive plates are found to give a significant inductive effect on RWM sensor measurement when RWM coils are activated

DC sensor compensations for RWM identification

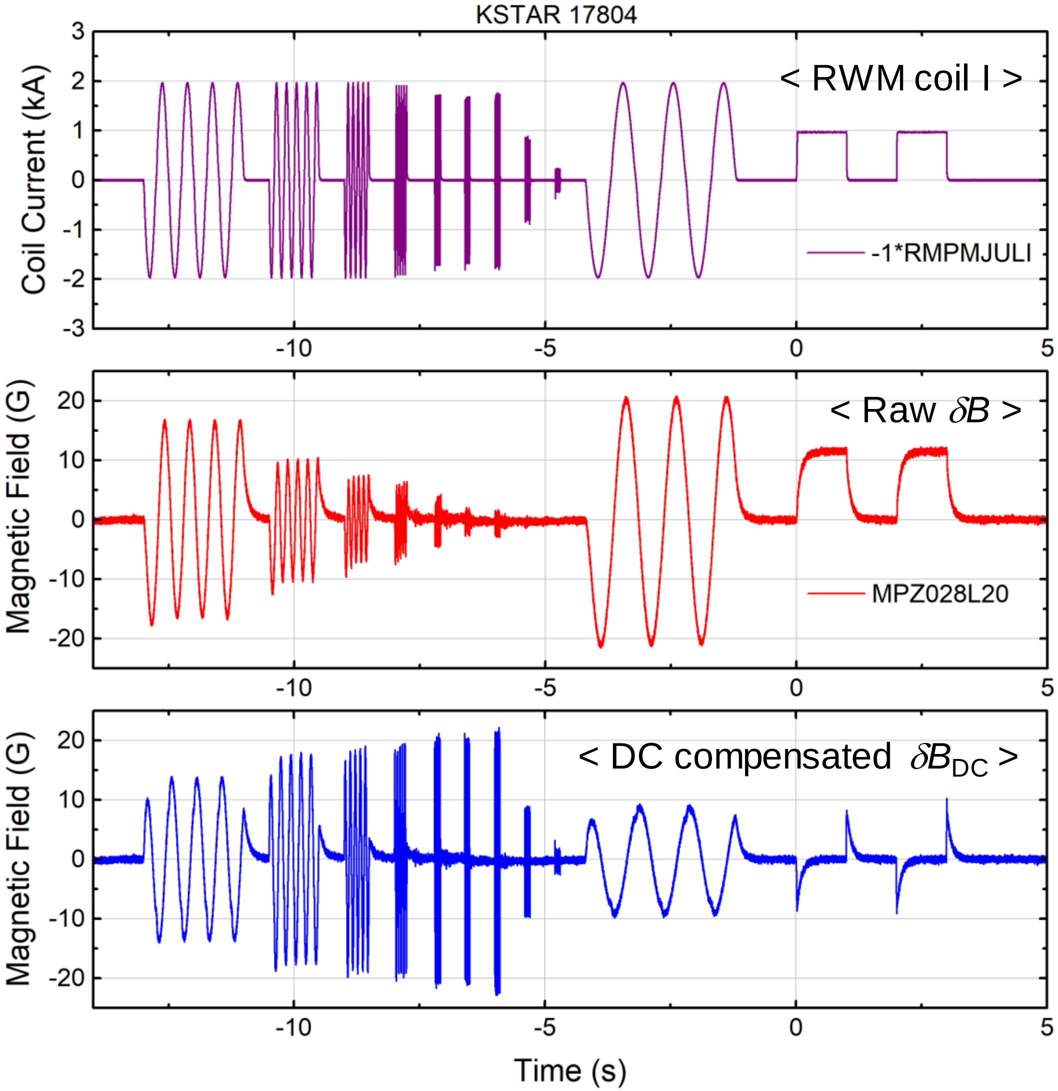

- Define the DC-compensated δB:

$$\delta B_{\mathrm{DC}} = \delta B_{\mathrm{COR}} - \sum_{j}^{N_{\mathrm{coil}}} M_j I_j$$

δB_{COR} : corrected δB by base-line subtraction, drift correction

- Significant inductive component still remains in δB_{DC} which can be compensated by using either:

  - Voltage loops on passive plates (not presently available in KSTAR)

  - RWM coil current (dI_{RWM}/dt) as vessel current sources

AC sensor compensation can eliminate the remaining δB components after the DC compensations

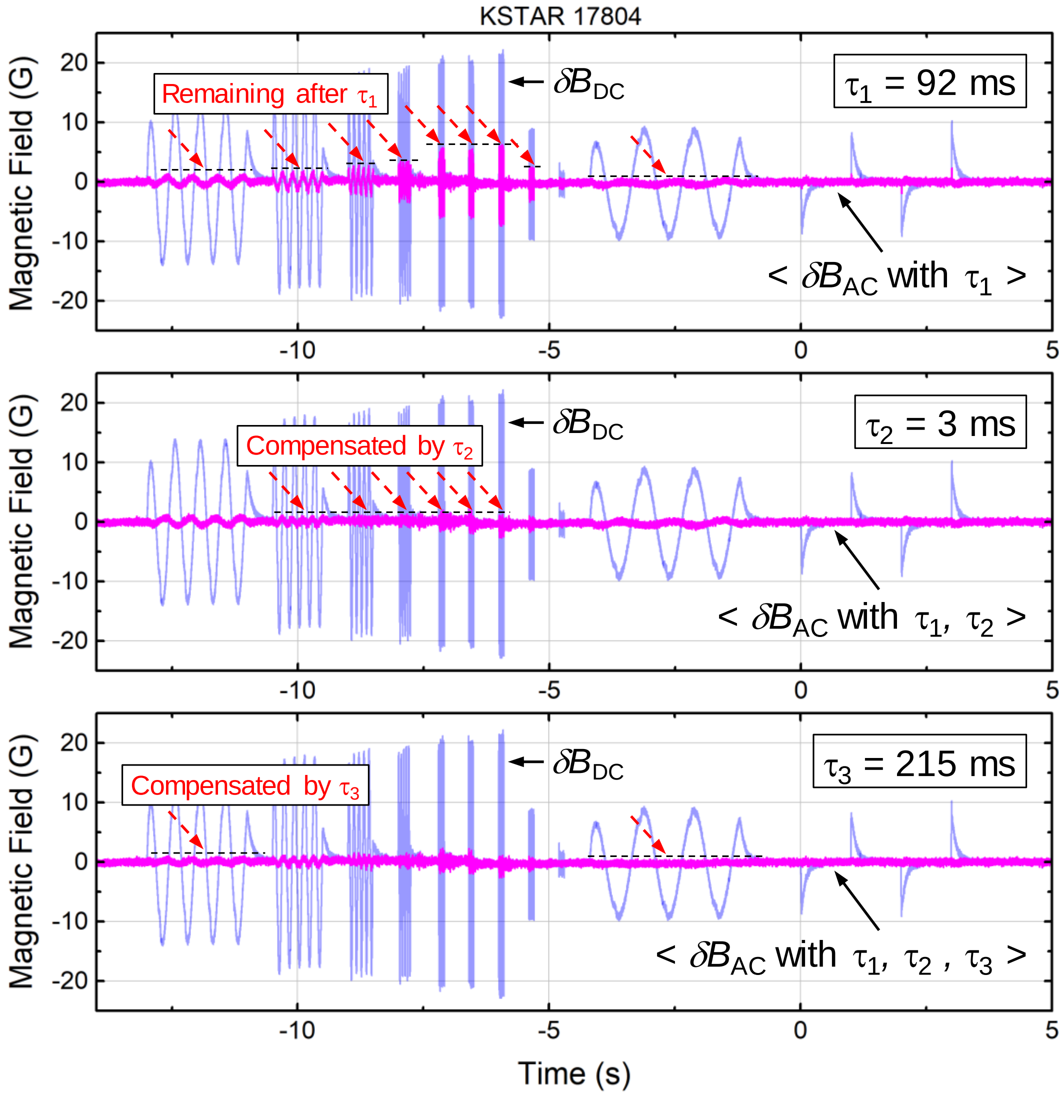

- Similar to NSTX, use low-pass-filtered (LPF) RWM coil currents as the source of the inductive δB
- Define the AC compensated δB:

$$\delta B_{\mathrm{AC}} = \delta B_{\mathrm{DC}} - \sum_{j}^{N_{\mathrm{coil}}} \sum_{k}^{N_{\tau}} p_{j,k} LPF\left(\frac{dI_{RWM,j}}{dt}; \tau_{AC,k}\right)$$

- The coefficient matrix p has max. 20 (N_{sensor}) x 12 (N_{coil}) x 3 (N_{τ}) = 720 elements
- LPF with 3 different τ values has been tested
- Tested τ set well compensates the inductive effect. For the entire RWM sensors, remaining $|\delta B|$ < 2 G after DC+AC compensations

Algorithms for mode identification (mode-ID)

- The magnetic perturbation has an amplitude (A_{RWM}) and phase (ϕ_{RWM})

$$B(\phi) = A_{RWM}\cos(\phi - \phi_{RWM})$$

- At the *i*-th sensor, the measured mode amplitude is:

$$B_i = A_{RWM}\cos(\phi_i - \phi_{RWM})$$
$$B_i = A_{RWM}\cos(\phi_{RWM})\cos(\phi_i) + A_{RWM}\sin(\phi_{RWM})\sin(\phi_i)$$
$$B_i = C_{RWM}\cos(\phi_i) + S_{RWM}\sin(\phi_i)$$

- Combine signals to form an amplitude and phase of the plasma 3D perturbation

$$\begin{bmatrix} B_1 \\ B_2 \\ \vdots \\ B_N \end{bmatrix} = \boxed{\begin{bmatrix} \cos(\phi_1) & \sin(\phi_1) \\ \cos(\phi_2) & \sin(\phi_2) \\ \vdots & \vdots \\ \cos(\phi_N) & \sin(\phi_N) \end{bmatrix}} \begin{bmatrix} C_{RWM} \\ S_{RWM} \end{bmatrix} = M \begin{bmatrix} C_{RWM} \\ S_{RWM} \end{bmatrix} \Rightarrow \begin{bmatrix} C_{RWM} \\ S_{RWM} \end{bmatrix} = M^{-1} \begin{bmatrix} B_1 \\ B_1 \\ \vdots \\ B_N \end{bmatrix} \Rightarrow \boxed{\begin{aligned} A_{RWM} &= \sqrt{C_{RWM}^2 + S_{RWM}^2} \\ \phi_{RWM} &= \operatorname{atan}\left(S_{RWM} / C_{RWM}\right) \end{aligned}}$$

M : mode-ID matrix (20 x 2) for KSTAR

- Convert the sensor fields at each time point to amplitude and phase
- Outputs passed within PCS to RWM feedback algorithms for control current request
- Algorithm is presently being implemented in KSTAR PCS for use in 2018

Measured amplitude and phase of slowly rotating MHD mode

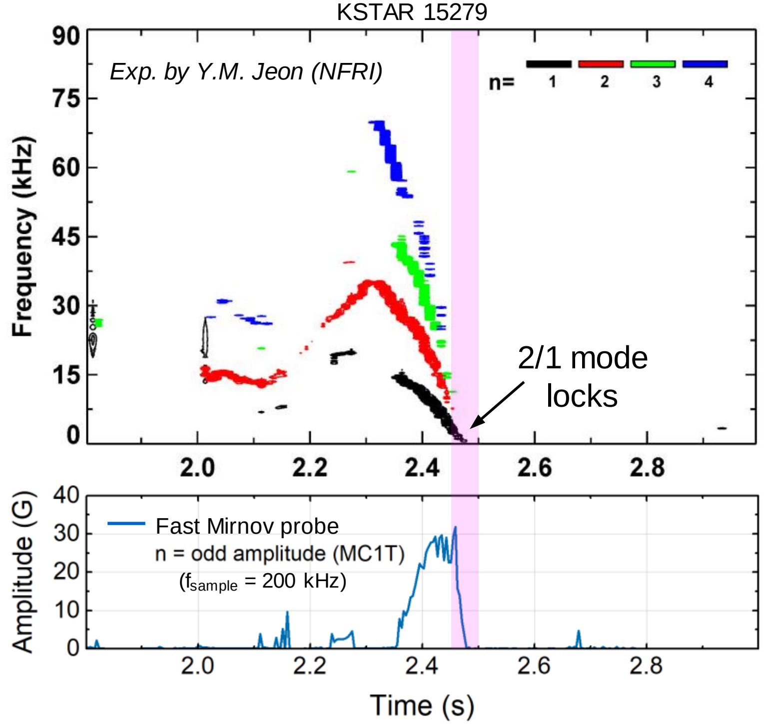

Toroidal magnetic probe spectrum and mode amplitude

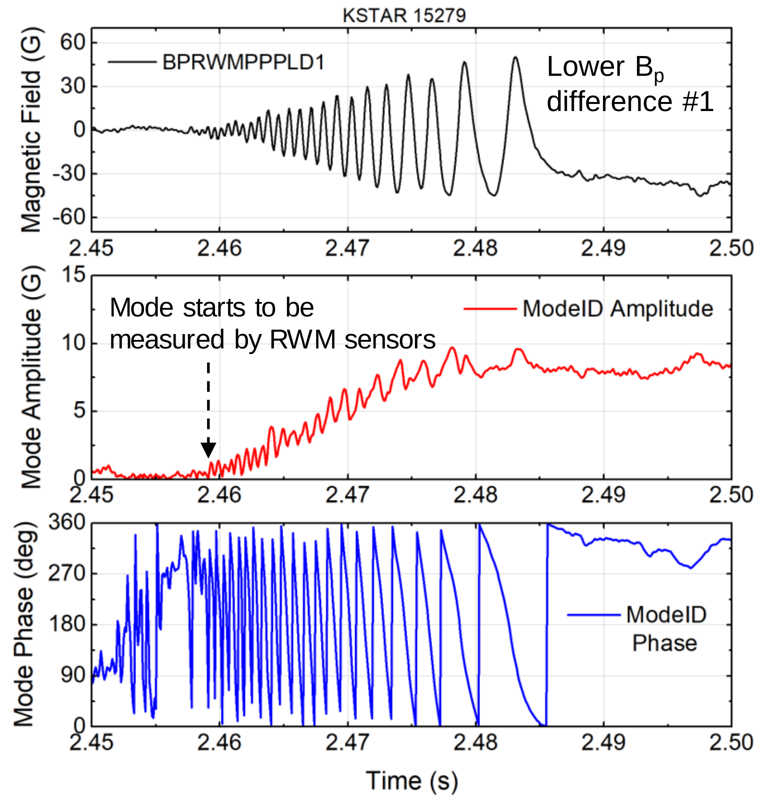

Measured mode amplitude and phase by mode-ID

- Since RWMs have yet to be measured on KSTAR, mode identification has been tested for slowly rotating tearing modes (w/o applied feedback)
- Used 10 B_p sensor differences (180º opposing sensor pairs) for n = 1 identification
- Mode identification well measures the evolution of n = 1 locking tearing mode

Conclusions and Next Steps

- KSTAR plasmas have exceeded the predicted ideal n = 1 no-wall limit
- Ideal and resistive stability of the achieved high β_N is analyzed
  - Kinetic EFIT with MSE constraints is used for accurate stability analysis
  - Achieved high β_N equilibria are subject to ideal n = 1 mode instability (DCON, M3D-C[1])
  - Resistive DCON analysis emphasizes the role of the pressure driven effects in the observed tearing stability
  - Kinetic RWM stability can explain the observed stability at high β_N (MISK)
- Development of algorithm for RWM identification
  - Significant δB induced mostly by the passive plate response is well compensated
- Next Steps
  - Improve stability analysis by employing the pressure driven terms calculated by TRANSP, and by further refinement in the kinetic EFIT reconstructions
  - Implement the developed mode-ID routines into the KSTAR PCS
  - Attempt experiments in 2018 to improve sustained high β_N, and probe MHD stability